This is the accepted version of the following article:
Taylor, A., Drahokoupil, J., Fekete, L., Klimša, L., Kopeček, J., Purkrt, A., . . . Mortet, V. (2016). Structural, optical and mechanical properties of thin diamond and silicon carbide layers grown by low pressure microwave linear antenna plasma enhanced chemical vapour deposition. *Diamond and Related Materials, 69*, 13-18. doi:10.1016/j.diamond.2016.06.014

This postprint version is available from http://hdl.handle.net/10195/67508

Publisher's version is available from http://www.sciencedirect.com/science/article/pii/S0925963516302163

This postprint version is licenced under a Creative Commons Attribution-NonCommercial-NoDerivatives 4.0.International.

Structural, optical and mechanical properties of thin diamond and silicon carbide layers by low pressure microwave linear antenna plasma enhanced chemical vapour deposition

*Andrew Taylor[1,2], Jan Drahokoupil[1], Ladislav Fekete[1], Ladislav Klimša[1], Jaromír Kopeček[1] Adam Purkrt[1], Zdeněk Remeš[1,2], Radim Čtvrtlík[3], Jan Tomáštík[3], Otakar Frank[4], Petr Janíček[5,6], Jan Mistrík[5,6], and Vincent Mortet[1,2]

[1] Institute of Physics of the Czech Academy of Sciences, Prague, Czech Republic

[2] Czech Technical University in Prague, Faculty of Biomedical Engineering, Kladno, Czech Republic

[3] Institute of Physics of the Czech Academy of Sciences, Joint Laboratory of Optics of Palacký University and Institute of Physics AS CR, Olomouc, Czech Republic

[4] J. Heyrovsky Institute of Physical Chemistry of the ASCR, v.v.i, Prague, Czech Republic

[5] Institute of Applied Physics and Mathematics, Faculty of Chemical Technology, University of Pardubice, Pardubice, Czech Republic

[6] Center of Materials and Nanotechnologies, Faculty of Chemical Technology, University of Pardubice, Pardubice, Czech Republic

KEYWORDS: Diamond, silicon carbide, adherence, mechanical properties, optical properties

ABSTRACT In this work, we detail the properties of thin silicon carbide and polycrystalline diamond layers grown by microwave plasma enhanced chemical vapour deposition with linear antenna delivery. Structural, mechanical and optical properties are compared for their potential use as transparent hard coatings. Silicon carbide layers exhibit mechanical properties comparable to thin diamond layers but with a significantly higher adhesion and lower optical absorption coefficient over a wide spectral range.

1. Introduction

Silicon carbide (SiC), as diamond, possesses a large number of outstanding properties, such as high hardness, high thermal conductivity, large band gap, wide wavelength range of transparency, chemical inertness with variable electrical conductivity by doping, etc. Hence, SiC and diamond thin films hold a wide range of promising mechanical, optical, optoelectronic, and electrical applications as an inert, hard, conducting or insulating, and transparent coating [1, 2]. Wide band gap thin layers would provide ideal transparent protective films on optical components. Additionally, when doped with boron, diamond thin films also hold promising electrochemical applications [3, 4]. However, these layers must exhibit low surface roughness, high adhesion and wear resistance in addition to high transparency and chemical inertness for long term applications. In this work, we detail and compare structural, mechanical, adhesion and optical properties of thin silicon carbide and diamond layers grown by microwave plasma enhanced chemical vapour deposition with linear antenna delivery.

2. Experimental:

Silicon carbide and diamond layers were deposited on {100} 20 mm^2 silicon wafers (ON Semiconductor Czech Republic, s.r.o) with an amorphous native oxide top layer and 10 mm^2 glass substrates (Corning Eagle XG) using a microwave plasma enhanced chemical vapour deposition system with linear antenna delivery (MW-LA-PECVD) [5, 6]. Prior to growth all substrates were ultrasonically cleaned in acetone and isopropyl alcohol. Substrates for diamond layer growth were seeded with a nano-crystalline diamond dispersion (NanoAmando®B) via spin coating, whereas silicon carbide layers were grown on unseeded substrates. All layers were deposited in a hydrogen rich, methane and carbon dioxide gas mixtures at low pressure with the same microwave power. Deposition conditions of silicon carbide and diamond layers are reported in Table I. As matter of fact, silicon carbide formation is not expected with the process gas mixture without a Si precursor. However, we recently demonstrate the presence of Si by optical emission spectroscopy in the MW-LA-PECVD system at low CO_2 concentrations and the consequent formation of silicon carbide due to the assumed plasma etching of the quartz tubes which form the vacuum to air interface in this system [5]. Substrate temperatures were monitored during deposition using a Williamson Pro 92-38 infrared pyrometer and thermocouples mounted in the substrate table. Both temperature measurement techniques were in agreement. Temperatures are noted in Table 1.

Morphological and structural properties of deposited layers were characterised by a Tescan FERA 3 scanning electron microscope optimised for observation of thin film morphology and thickness measurement in cross-section. Ambient atomic force microscopy using a Dimension Icon (Bruker) in peak force tapping mode with Tap150AL-g tips optimised for surface topography and surface roughness was measured on a 3×3 mm^2 surface area.

The crystalline structure of deposited layers was characterised by X-ray diffraction methods using a PANalytical X´Pert PRO diffractometer with a Co anode (λ = 0.1789 nm) with different configurations. The diamond layers were measured with the line focus in a parallel beam geometry with a Goebel mirror in the primary beam and a parallel plate collimator (0.09°) in the diffracted beam by 2θ-scan with a fixed angle of incident equal to 2° whereas SiC layers were measured with line focus in Brag-Brentano geometry using divergent slits and linear detector (X´Celerator). The pole figures and ψ-scans of SiC were also measured with a point focus on ATC-3 texture cradle.

Raman spectra were recorded by a LabRAM HR (Horiba Jobin-Yvon) spectrometer coupled to an Olympus BX microscope with a 100x objective. He-Ne laser with 1.96 eV (633 nm) energy was used as excitation with the power at the sample of 8 mW. 600 grooves/mm grating and a confocal hole of 50 µm was used. Spectra were background-corrected using the spectrum of the glass substrate as the baseline.

The mechanical and tribological properties were measured by nanoindentation and scratch test techniques at room temperature using a fully calibrated NanoTest instrument (MicroMaterials). Nanoindentation experiments were performed with a sharp Berkovich indenter in a load controlled mode. Taking into account the thickness of the films, their roughness, ability to calibrate the indenter tip at shallow depths and the requirement of full plasticity beneath the indenter, two indentation loads of 1.0 and 1.5 mN [7] were chosen for determination of the stability of mechanical properties of the films with increasing depth and also to validate the used experimental setup. Progressive nanoscratch tests were performed in a 3 step procedure: 1-topography, 2-scratch and 3-topography for two maximum loads (300 mN and 500 mN). The initial and final topography measurements were performed at a load of 0.02 mN to avoid any

wear. During the scratch procedure the initially constant topographic load of 0.02 mN was applied over the first 50 μm and then ramped to the maximum load at constant loading rate of 7.8 and 13 mN/s respectively. All scans were performed with a scan speed of 10 μm/s over a total scan length of 450 μm. Nano-wear tests, i.e. multi-pass scratch tests were performed at a constant load of 20 mN by alternating scratch and topography passes every two scratches to monitor surface degradation, 16 passes were carried out in total. All evaluations of scratch tests were performed on the basis of the indenter load-depth records and analysis of the residual scratch tracks. Laser scanning confocal microscope LEXT OLS 3100 (Olympus) was used for high-resolution imaging.

Index of refraction and absorption coefficient of deposited layers were measured from UV to near infrared (250 nm to 1700 nm) using photothermal deflection spectroscopy (PDS) [8] and ellipsometry. The optical transmittance, reflectance and absorptance spectra were measured simultaneously in the broad spectral range from ultraviolet to near infrared in a dual beam setup. The absorptance down to 10^{-4} was measured by the absolute photothermal deflection spectroscopy (PDS) normalised via the signal of the highly absorbing black coating [9]. Ellipsometry measurements were carried out using a VASE ellipsometer (Woollam) from 190 nm to 2400 nm. Spectra were recorded in reflection for three angles of incidence (60, 65, and 70 degrees) and were analysed simultaneously with nearly normal reflectivity and transmission measured with the same instrument.

3. Results and discussion

Figure 1 shows the surface morphology of diamond and SiC thin films observed by scanning electron microscopy. Diamond layers exhibit polycrystalline columnar facetted grains, typical of

the van der Drift growth mode. In comparison, silicon carbide layers show a fine columnar structure and a smooth surface. This difference in surface morphology is highlighted by the large difference in root mean square roughness of the diamond layers (18 nm for a thickness of 400 nm) and the SiC layers (2 nm for a thickness of 390 nm) as measured by AFM .

The (111) textured cubic SiC with no in plane preferred orientation has been identified by X-ray diffraction (see Figure 2a). The XRD pattern shows one diffraction line at ca. 41.5° indicating a strongly textured thin film which can be assigned to the cubic (111) or hexagonal (002) structure of SiC. The crystalline structure of SiC was resolved by pole figures and ψ-scans measurements. The pole figure at ca. 58.5° which corresponds to the 012 diffraction of a hexagonal structure does not show any peaks. On the other hand, the pole figure at ca. 70.6°, which corresponds to the 220 diffraction of cubic structure, shows a broad ring with a maximum at $\psi \approx 35°$, which corresponds to 35.26°, i.e. the angle between [111] and [220] directions for a cubic structure (see Figure 2b). Furthermore, the ψ-scan at 41.5° shows a secondary maximum close to 70°, which correspond to the angle between the [111] and [-111] direction. These results are consistent with transmission electron microscopy results reported in [5]. In comparison, the polycrystalline nature of diamond is clearly shown on the X-ray diffraction diagram on Figure 2a.

The Raman spectrum of diamond layers clearly exhibits the 1332 cm^{-1} zone-centre phonon diamond Raman peak together with bands at 1140 and 1500 cm^{-1}, related to trans-poly-acetylene [10]. Figure 3 shows the baseline-corrected Raman spectrum of the SiC thin layer grown on a glass substrate. Several features can be discerned. The Raman bands corresponding to the transverse (TO) and longitudinal (LO) optical phonons at ~ 782 and 945 cm^{-1} are the typical markers of the β-SiC. However, in the case presented in Figure 3, the bands are broad and

downshifted compared to crystalline β-SiC [11]. The downshift is more pronounced for the LO band (nominally at 966 cm^{-1}) compared to the TO band (nominally at 795 cm^{-1}). The downshift indicates the presence of other SiC polytypes as inhomogeneities in the lattice [12]. Furthermore, the presence of additional bands at ~ 890 and 720 cm^{-1} is attributed to amorphous SiC [11] and the features below 600 cm^{-1} are assigned to acoustic modes, which is the signature of disorder in SiC [12]. The Raman spectrum thus clearly evidences the nano-crystalline and disordered character of the grown SiC. On the other hand, no Raman bands attributable to sp^2 or sp^3 (disordered) carbon in the range at 1300-1600 cm^{-1} could be seen, indicating that SiC is indeed the only carbon compound grown. These results are supported by Fourier Tranform Infrared transmission measurements in 400-4000 cm^{-1} range which show only a Si-C absorption peak at 800 cm^{-1}.

Hardness and elastic modulus of thin diamond and SiC layers together with the reference (100) Si crystalline substrate, measured with an indentation load of 1.0 mN, are reported in Figure. 4. Their values can be considered to be film dominated as the maximum indentation depths do not exceed 10% of the film thickness [13].This is supported by the same determined values at higher load (1.5 mN). The high hardness value of ~38 GPa of a 360 nm thick SiC carbide layer is consistent with other reported values for stoichiometric SiC thin films [14] and in agreement with hardness values of single crystal α-SiC (36 GPa) and β-SiC (32 GPa) [15]. Note that the larger spread of hardness and elastic modulus values for diamond layers compared to SiC layers are attributed to different surface morphologies. In comparison diamond layers with a similar thickness (300 nm) exhibit a lower measured hardness (33 GPa). However, elastic modulus values of diamond and SiC layers are nearly equal. The measured hardness value lies in the range of the possible values for diamond layers [16, 17], though values approaching single

crystal diamond were reported [18]. It should be noted that the hardness of the diamond films is strongly affected by the portion of the amorphous phase surrounding the diamond grains, containing both the sp^2 and sp^3 hybridized carbon.

The on-load depth and topography data of diamond and SiC layers for the progressive scratch tests are shown in Figure 5a. Figure 5b shows that the worn surface morphology is dominated by plastic deformation at low loads while increasing the normal load, faint cracking inside the wear track followed by chipping at the edges of the scratch grooves occurs. Although the on-load depths are rather similar there is an evident difference in critical loads, i.e. the onset of critical failure of the layers. Diamond layers fail at a load of 32 mN, while the critical load for SiC is 292 mN. These results show the significant adhesion and/or cohesion improvement at the silicon/SiO_2/silicon carbide interface compared to the diamond layers on Si/SiO_2 substrates seeded with diamond nano-particles due to the weak chemical bond between particles and substrate.

Although the hardness and reduced elastic modulus values of diamond and SiC layers are close, their ability to withstand the repetitive scratch loads differ significantly. Figure 6 shows the on-load and topography depth records of diamond and SiC layers. Smooth profiles for all the passes are clearly seen for the SiC layers, while a sudden drop in penetration depths and development of surface roughness are clearly observed for diamond layers. The adhesion of diamond layers fails during the 4th pass while no catastrophic damage of SiC layers is observed, even after additional experiments performed at a load of 75 mN.

Figure 7 compares optical properties, i.e. refractive index and absorption coefficient of SiC and diamond layers, measured by ellipsometry and transmission/reflexion/PDS spectroscopies. Both

types of layers are transparent over a wide spectral range in the visible and near infrared regions (400 nm – 1 um). The refractive index of SiC layers n_{SiC}, is lower than the β-SiC bulk value $n_{\beta\text{-}SiC}$ (n_{SiC} = 2.407 vs. $n_{\beta\text{-}SiC}$ = 2.6434 at 600 nm)[19]. Similarly, the refractive index of diamond layers n_{NCD}, is lower than the diamond bulk value n_D (n_{NCD} = 2.230 vs. n_D = 2.4133 at 600 nm) [20]. SiC layers show a slightly lower absorption coefficient than diamond layers in the visible range. The increase of the optical absorption coefficient of a doped semiconductor is related in the infrared region to the absorption on free carriers. There is no clearly defined optical absorption edge in the UV region. An advantage of the PDS is the direct measurement of the optical absorption measurement by detecting the increase of the temperature suppressing the effects of optical scattering. Thus, once the film thickness and the index of refraction are known, the optical absorption coefficient is calculated directly from the optical absorption measured by PDS at each wavelength independently without being restricted by the use of parametric models. Noticeably, ellipsometry overestimates the absorption coefficient with respect to the results determined by PDS. Nevertheless, it should be mentioned that for low values of absorption coefficients ($<10^5$ cm^{-1}) ellipsometry is no more sensitive to material absorption.

4. Conclusion

Silicon carbide and diamond thin layers have been deposited by a microwave plasma enhanced chemical vapour deposition system with linear antenna delivery at low temperature. Their structural, optical and mechanical properties have been measured and compared for their potential use as hard optical protective coating applications. The thin (< 500 nm) diamond layers exhibit columnar well facetted grains typical of microcrystalline CVD diamond growth, often referred to as nano-crystalline diamond (NCD), which are in contrary to smooth ultra nano-

crystalline diamond (UNCD) with small grains and high secondary nucleation rates [21]. SiC layers display a low surface roughness which does not change with thickness, which is opposed to the diamond layer's growth. Measured values for SiC layer hardness and elastic modulus are comparable with the diamond layers but with a significantly higher adhesion and wear resistance. SiC layers exhibit an index of refraction close to bulk diamond and show a lower absorption coefficient than diamond layers in the visible range.

AUTHOR INFORMATION

Corresponding Author

*Corresponding author. Tel: (+420) 266 052 634. E-mail: taylor@fzu.cz (Andrew Taylor)

Author Contributions

The manuscript was written through contributions of all authors. All authors have given approval to the final version of the manuscript.

ACKNOWLEDGMENT

We acknowledge the financial support from the Technology Agency of the Czech Republic, Grant No. TA03010743, the Czech Science Foundation project 13-31783S, project LD14011 (HINT COST Action MP1202), SAFMAT LM2015088 and LO1409, and the J.E. Purkyne fellowship awarded to V. Mortet by Academy of Sciences of the Czech Republic.

REFERENCES

1. Chakrabarti, K.; Chakrabarti, R.; Chattopadhyay, K.K.; Chaudhrui, S.; Pal, A.K. Nano-Diamond Films Produced from CVD of Camphor Diam. Relat. Mater. 7 (1998) 845 - 852

2. Guruvenket, S.; Azzi, M.; Li, D.; Szpunar, J.A.; Martinu, L.; Klemberg-Sapieha, J.E.; Structural, Mechanical, Tribological, and Corrosion Properties of a-SiC:H Coatings prepared by PECVD Surface & Coatings Technology 204 (2010) 3358–3365
3. Luong, J.H.; Male, K.B.; Glennon, J.D. Boron-doped Diamond Electrode: Synthesis, Characterization, Functionalization and Analytical Applications. Analyst. 2009 Oct 134 (10) 1965-79
4. Kavan, L.; Vlckova Zivcova, Z.; Petrak, V.; Frank, O;. Janda, P;. Tarabkova, H;. Nesladek, M;. Mortet, V. Boron-doped Diamond Electrodes: Electrochemical, Atomic Force Microscopy and Raman Study towards Corrosion-modifications at Nanoscale Electrochimica Acta 179 (2015) 626–636
5. Taylor, A.; Ashcheulov, P.; Čada, M.; Fekete, L.; Hubík, P.; Klimša, L.; Olejníček, J.; Remeš, Z.; Jirka, I.; Janíček, P.; Bedel-Pereira, E.; Kopeček, J.; Mistrík, J.; Mortet, V. Effect of Plasma Composition on Nanocrystalline Diamond Layers deposited by a Microwave Linear Antenna Plasma-Enhanced Chemical Vapour Deposition System Phys. Status Solidi A 212 (2015) 2418
6. Fendrych, F.; Taylor, A.; Peksa, L.; Kratochvilova, I.; Vlcek, J.; Rezacova, V.; Petrak, V.; Kluiber, K.; Fekete, L.; Liehr, M.; Nesladek, M. Growth and Characterization of Nanodiamond Layers prepared using Plasma Enhanced Linear Antennas Microwave CVD System, J. Phys. D: Appl. Phys. 43 (2010) 374018 (6pp)
7. Fischer-Cripps, A.C. Nanoindentation Springer; 2004 ISBN 978-1-4757-5943-3
8. Jackson, W.B.; Amer, N.M.; Boccara, A.C.; Fournier D. Photothermal Deflection Spectroscopy and Detection Appl. Opt. 20 (1981) 1333–1344
9. Remes, Z.; Pham, T. T.; Varga, M.; Kromka, A.; Mao, H. B. Carbon Coatings Prepared by Magnetron Sputtering and Microwave Plasma Enhanced Chemical Vapor Deposition Measured by the Photothermal Deflection Spectroscopy Advanced Science, Engineering and Medicine, Volume 7, Number 4, April 2015, pp. 321-324(4)
10. Ferrari, A.C.; Robertson, J. Origin of the 1150 cm^{-1} Raman mode in nanocrystalline diamond, Phys. Rev. B 63, 121405(R) (2001).
11. Havel, M.; Colomban, P. Skin/Bulk Nanostructure and Corrosion of SiC-based Fibres: a Surface Rayleigh and Raman study J. Raman Spectrosc. 2003; 34: 786–794

12. Nakashima, S.; Harima, H.; Raman Investigation of SiC Polytypes phys. stat. sol. (a) 162, 39 (1997)
13. Burnett, P.J.; Rickerby, D. S. The mechanical properties of wear-resistant coatings: I: Modelling of hardness behaviour, Thin Solid Films 148 (1987) 41-50.
14. Bayne, M.A.; Kurokawa, Z.; Okorie, N.U.; Roe, B.D.; Johnson, L.; Moss, R.W. Microhardness and other properties of Hydrogenated Amorphous Silicon Carbide Thin Films formed by Plasma-Enhanced Chemical Vapor Thin Solid Films, 107 (1983) 201
15. Kulikovsky, V.; Vorlíček, V.; Boháč, P.; Stranyánek, M.; Čtvrtlík,R;. Kurdyumov, A. Hardness and elastic modulus of amorphous and nanocrystalline SiC and Si films, Surf. Coat. Technol. 202 (2008)
16. Henda, R.; Alshekhli, O.; Howlader, M.; Deen, J. Nanocrystalline Diamond films prepared by Pulsed Electron Beam Ablation on Different Substrates Journal of Materials Research, available on CJOAugust 2015. doi:10.1557/jmr.2015.254
17. Bogus, A.; Gebeshuber, I.C.; Pauschitz, A.; Manish, R.; Haubner, R. Micro- and Nanomechanical Properties of Diamond Film with Various Surface Morphologies Diamond & Related Materials 17 (2008) 1998–2004
18. Cicala, G.; Magaletti, V.; Senesi, G.S.; Carbone, G.; Altamura, D.; Giannini, C.; Bartali, R. Superior Hardness and Young's modulus of Low Temperature Nanocrystalline diamond coatings Materials Chemistry and Physics 144 (2014) 505-511
19. Shaffer, P. T. B. Refractive Index, Dispersion, and Birefringence of Silicon Carbide Polytypes Appl. Opt. 10 (1971) 1034.
20. Palik, E. D. Handbook of Optical Constants of Solids, Volume 1, ISBN: 978-0-08-0547213
21. Williams, O.A.; Daenen, M.; D'Haen, J.; Haenen, K.; Maes, J.; Moshchalkov, V.V.; Nesládek, M.; Gruen, D.M. Comparison of the growth and properties of ultrananocrystalline diamond and nanocrystalline diamond. Diamond & Related Materials 15 (2006) 654–658

	Diamond	SiC
Microwave power	2 × 3 kW	2 × 3 kW
Methane concentration	5%	4.2%
Hydrogen concentration	92%%	95.75%
Carbon dioxide concentration	3%	0.05%
Process pressure	0.3 mbar	0.3 mbar
Substrate temperature	520 °C	520 °C
Deposition rate	50 nm/h	33 nm/h

Table 1: Deposition conditions of silicon carbide (SiC) and diamond layers by microwave plasma enhanced chemical vapour deposition system with linear antenna delivery.

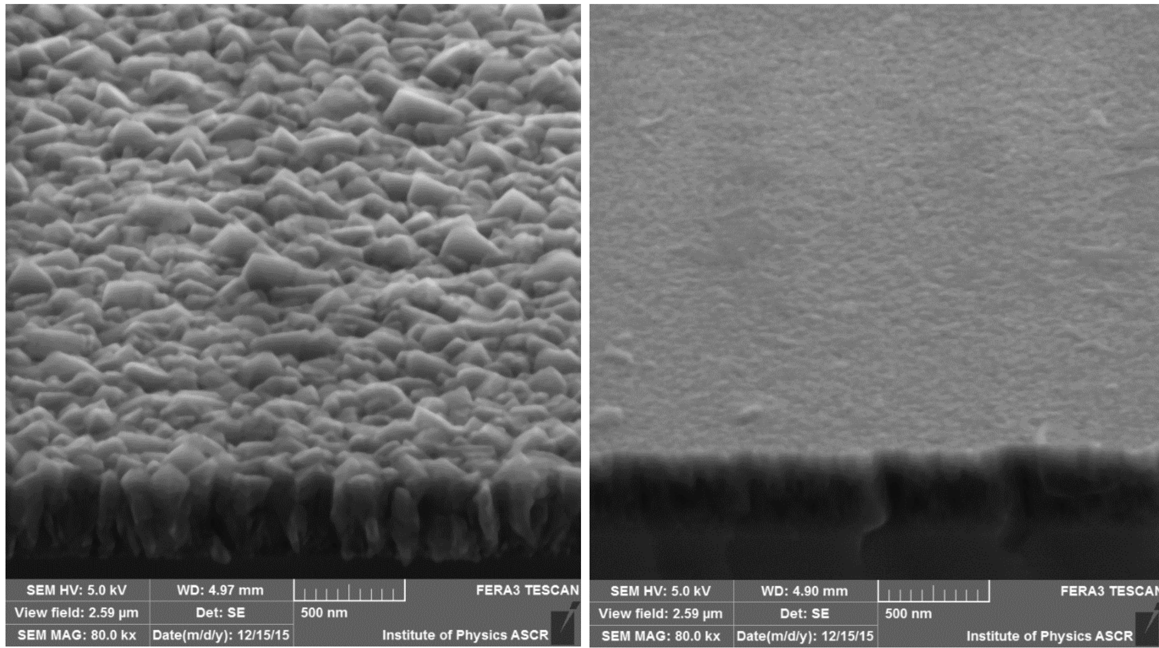

Figure 1: Scanning electron microscopy images of diamond (left) and silicon carbide (right) layers.

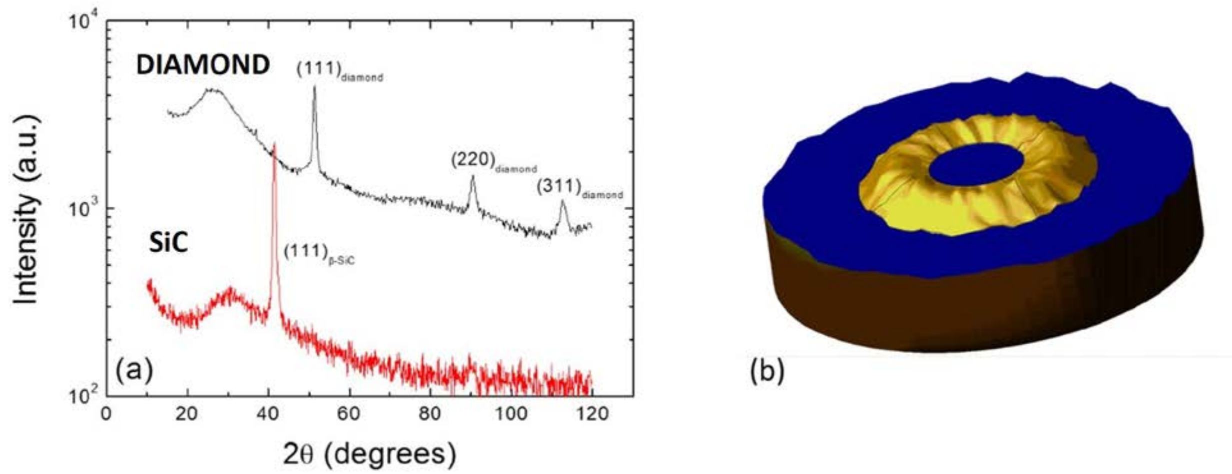

Figure 2: (a) X-ray diffraction diagram of diamond and silicon carbide (SiC) layers, (b) , pole figure at ca. 70.6° (220 diffraction of cubic structure) showing a broad ring with maximum at $\psi \approx$ 35° which corresponds the angle between [111] and [220] directions of β-SiC.

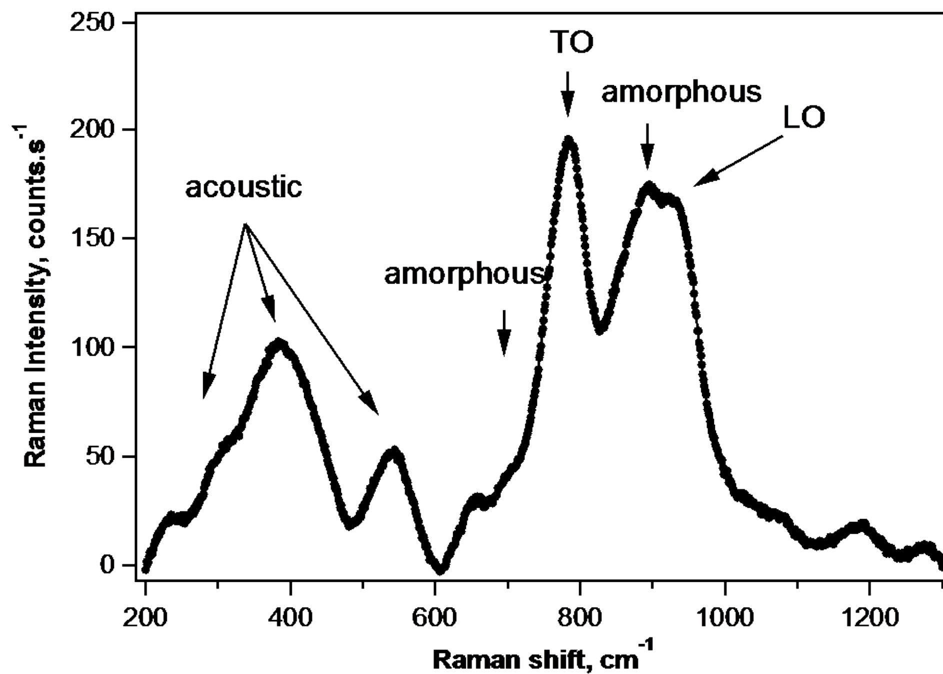

Figure 3: Raman spectrum of the SiC layer grown on a glass substrate. The spectrum is baseline-corrected using the glass substrate as the background for subtraction. Laser excitation energy is 1.96 eV.

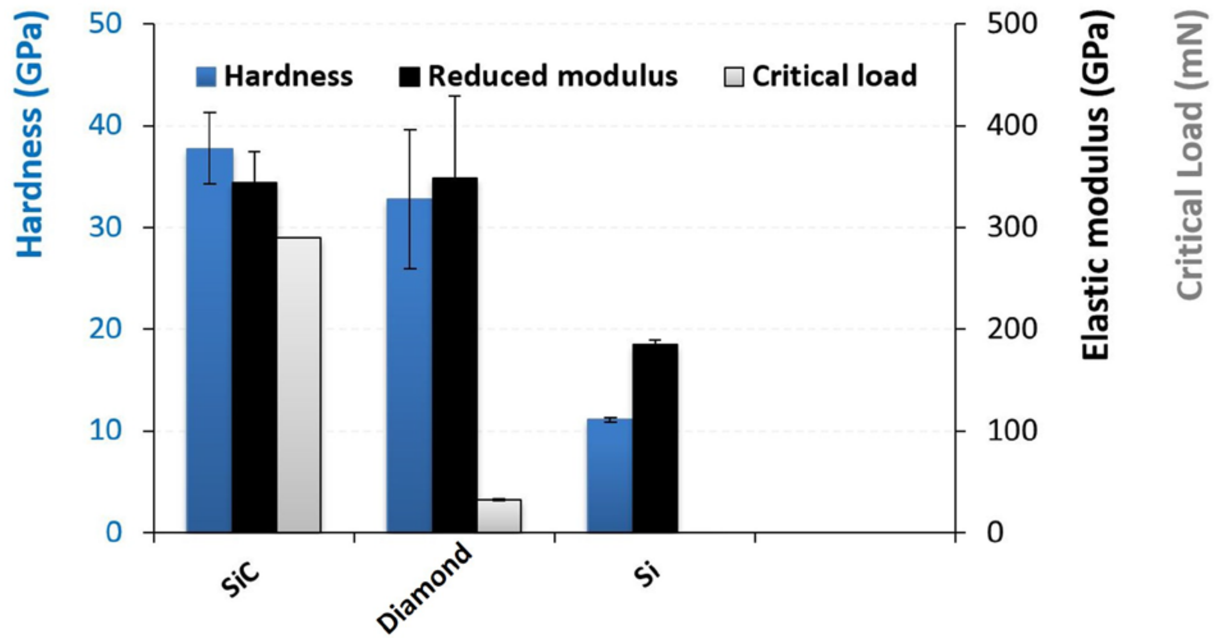

Figure 4: Hardness, reduced elastic modulus and critical load measurements of silicon carbide (SiC) and diamond layers compared to silicon (Si) reference.

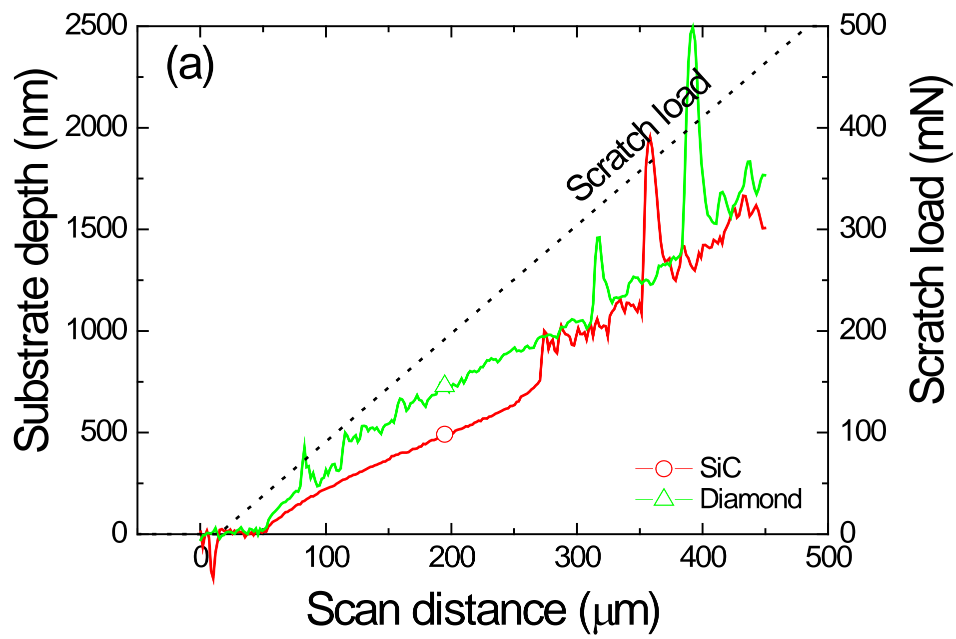

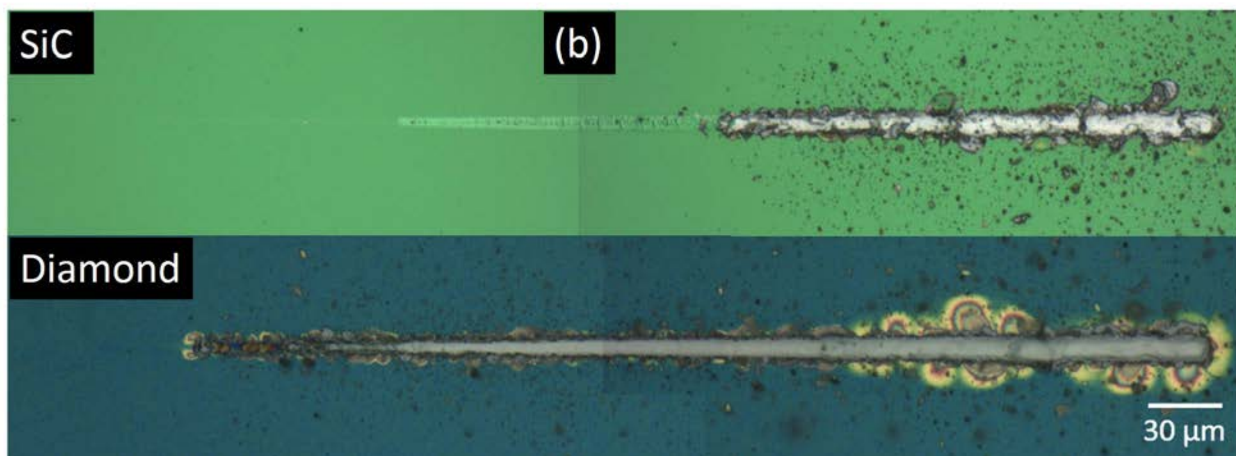

Figure 5: (a) Comparison of the on-load depth for SiC and diamond layers measured by scratch test method and (b) corresponding residual scratch grooves.

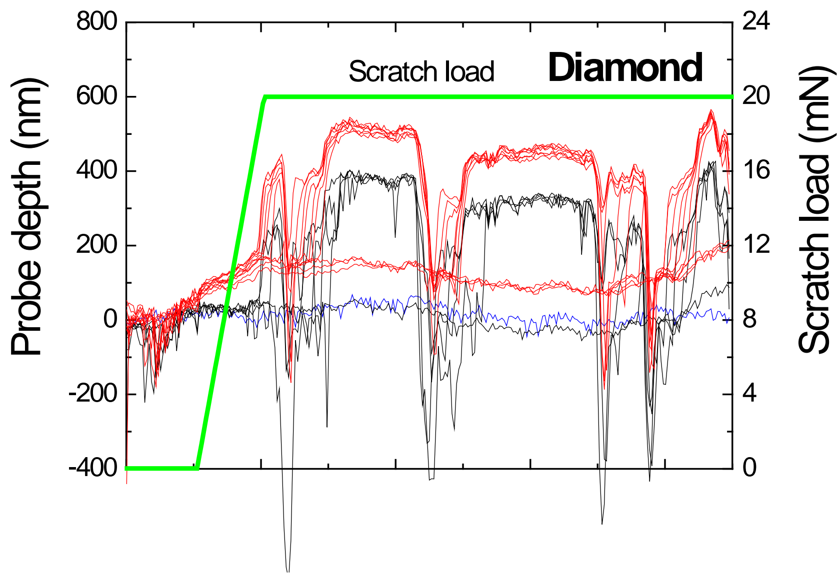

Probe depth (nm)
Scratch load (mN)
Scratch load
Diamond
800
600
400
200
0
-200
-400
24
20
16
12
8
4
0

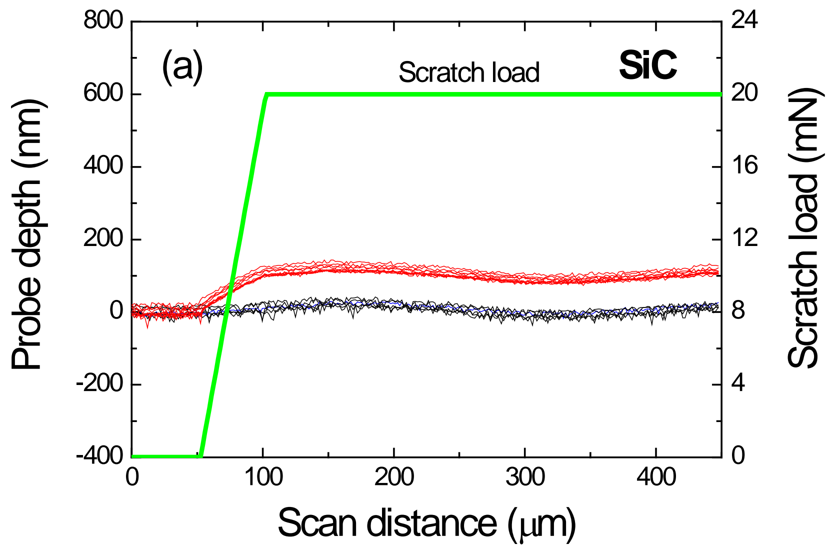

(a)
Scratch load
SiC
Probe depth (nm)
Scratch load (mN)
Scan distance (μm)
800
600
400
200
0
-200
-400
24
20
16
12
8
4
0
0
100
200
300
400

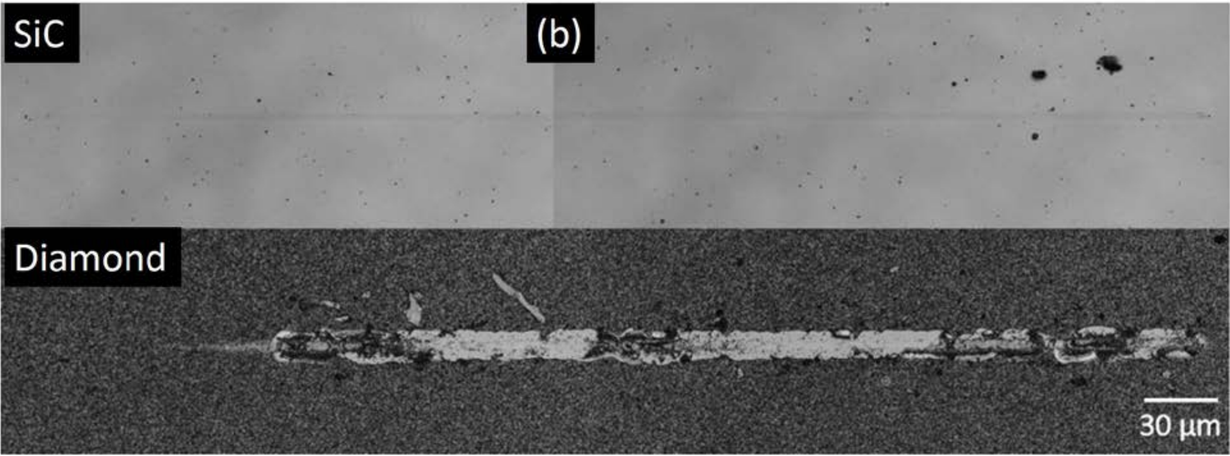

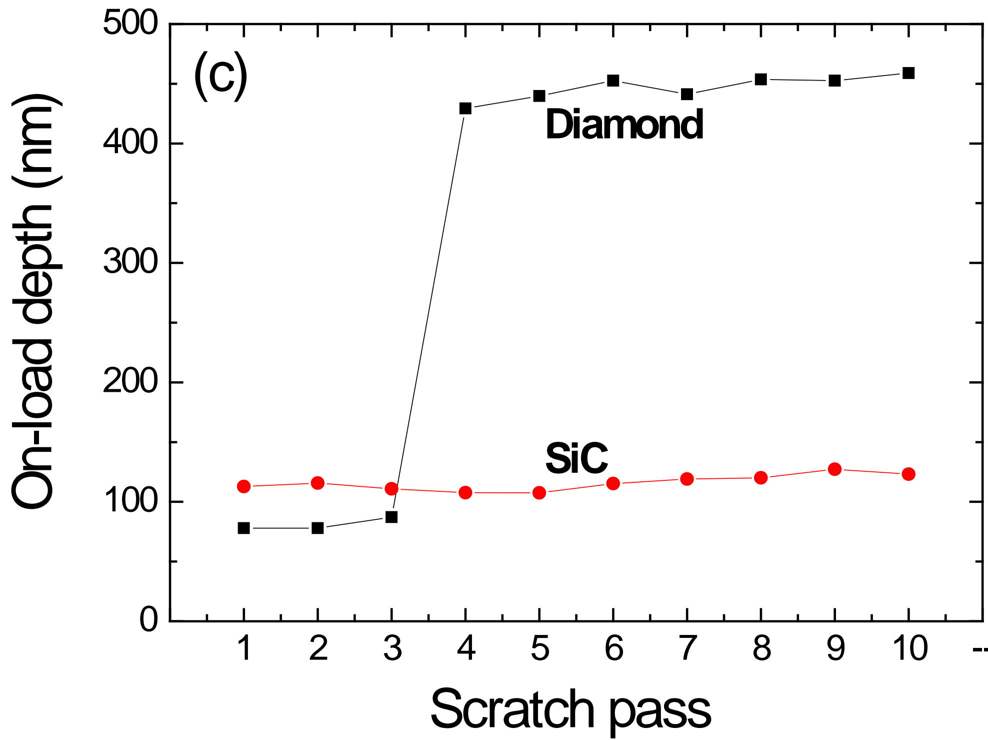

Figure 6: Multi-pass wear test's depth profiles (a) on-load and topography records, (b) residual wear tracks and (c) on-load depths evolution at the distance of 200 µm from the beginning of the test.

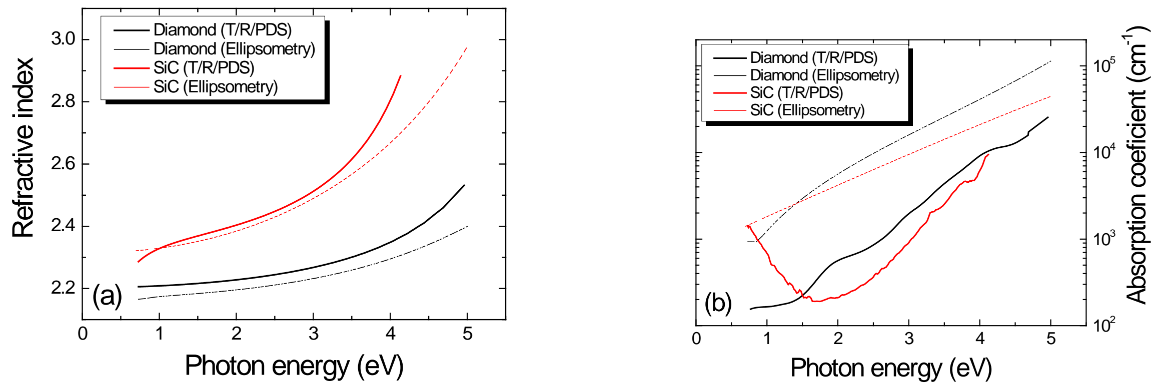

Figure 7: Comparison of refractive index (a) and absorption coefficient (b) of diamond and silicon carbide (SiC) layers deposited by MW-LA-PECVD measured by transmission, reflexion and photo-thermal deflection (T/R/PDS) method and ellipsometry.